электромагнитного поля // Изв. вузов Электромеханика. – 1992. – № 5. – С. 11–17. 4. Васьковский Ю.Н., Шинкаренко В.Ф. Математическое моделирование и исследование многороторных электромеханических преобразователей // Техническая электродинамика. – 2001. – № 2. – С. 41–46. 5. Васьковский Ю.Н. Моделирование электромашинного генератора импульсов тока с учетом нелинейности его электромагнитных связей // Техническая электродинамика. – 1992. – № 3. – С. 61–67. 6. Фильц Р.В. Математические основы теории электромеханических преобразователей. – К., 1979. – 206 с.

Ivo Doležel, Roman Hamar[*], Pavel Karban[*], Bohuš Ulrych[*]
Institute of Electrical Engineering, Czech Academy of Sciences, Prague, Czech Republic
[*] Faculty of Electrical Engineering, University of West Bohemia, Pilsen, Czech Republic

INTEGRAL AND SPECIAL METHODS IN MODELLING OF 3D ELECTRIC FIELDS

Computation of large electric fields in complicated 3D arrangements (especially with geometrically incommensurable subregions) by classic numerical techniques based on differential methods often fails due to lack of boundary conditions and problems with meshing. For some of these cases the paper offers integral or special approach. Particular algorithms are illustrated on two examples whose results are discussed.

Introduction. Investigation of large electric fields containing charged conductors of general 3D shapes is uneasy. Due to complex arrangements the analytical methods are practically inapplicable, and also classic numerical methods do not often lead to acceptable results. FDM- or FEM-based techniques may fail because of lack of the boundary conditions and severe problems with meshing (thin conductors versus large volume of ambient air). In such cases, integral [1, 2] and special methods can be used to cope with the task.

The integral techniques are in this case based on solution of a system of the first-kind Fredholm equations providing distribution of surface charge. Their analysis is supplemented with computation of the electric field between two generally placed charged cubes.

As known, corresponding weakly singular kernel functions are integrable only over 2D regions. This is in accordance with the physical reality because every conductor is characterised by nonzero surface. But discretisation of such surfaces often leads to very large system of equations whose processing on common PCs may be unfeasible.

For such cases the paper offers another alternative method suitable for mapping fields generated, for example, by a system of thin charged conductors of any shape in 3D domain. These conductors are first replaced by infinitely thin filaments and these are again replaced by sets of point charges located along helicoidal curves surrounding them. Their values are calculated on the condition that potential at the place of any filament is equal to potential of the corresponding conductor. The field quantities at any point in the area may then easily be calculated from the Coulomb law. Even this technique is illustrated on an example.

Integral model. Consider a system of n mutually electrically isolated well conductive metal conductors C_1, C_2,…, C_n carrying constant electric potentials φ_1, φ_2,…, φ_n (Fig. 1). The system is placed in a homogeneous medium of relative permittivity ε_r. Dimensions of the conductors are finite and their surfaces smooth by parts. It is necessary to map the electric field in the area of the conductors.

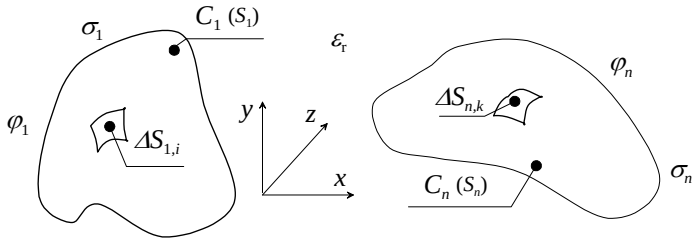

Fig. 1. General arrangement of the charged bodies

The first step is to find functions $\sigma_i(S_i)$, $i = 1, 2,\ldots, n$, describing the distribution of electric charges along surfaces S_i of conductors C_i. This is realised by solution of a system of the first-kind Fredholm integral equations in the form

$$\varphi_i(P) = \frac{1}{4\pi\varepsilon_0\varepsilon_r} \cdot \sum_{j=1}^{n} \int_{S_j} G(\boldsymbol{r}_P, \boldsymbol{r}_Q) \cdot \sigma_j(S_j)\,\mathrm{d}S, \quad P \in S_i,\ Q \in S_j,\ \ i, j = 1,\ldots,n \tag{1}$$

with weakly-singular kernel functions

$$G(\boldsymbol{r}_P, \boldsymbol{r}_Q) = \frac{1}{|\boldsymbol{r}_P - \boldsymbol{r}_Q|} \tag{2}$$

where P is the reference point and Q is variable point that passes through all surfaces S_j, $j = 1, 2,\ldots, n$. Discretised form of (1) reads (each surface being covered by N_i elements, $i = 1,\ldots, n$)

$$\varphi_i(P) = \frac{1}{4\pi\varepsilon_0\varepsilon_r} \cdot \sum_{j=1}^{n} \sum_{k=1}^{N_j} \int_{\Delta S_{j,k}} G(\boldsymbol{r}_P, \boldsymbol{r}_Q) \cdot \sigma\,\mathrm{d}S, \quad P \in S_i,\ Q \in S_j,\ \ i, j = 1,\ldots,n. \tag{3}$$

The basic advantage of the function $G(\boldsymbol{r}_P,\boldsymbol{r}_Q)$ is its integrability in 2D. Solvability of the system (1) and unambiguousness of the continuous model was proved in [3]. Discretisation is performed in the standard manner. The surfaces are approximated by triangular or quadrilateral (and generally unstructured) meshes. Real distribution of the charge density in particular cells is substituted by polynomial functions. Proper and improper integrals are calculated analytically for both triangular and rectangular cells.

The second step is to find the field quantities (potential, electric field strength, partial or total capacitances etc.) by means of relatively simple integral expressions.

Illustrative example. Consider two charged cubes in a position depicted in Fig. 2 placed in the air. The length of the edge of both cubes is 0.02 m and the distance between their centres 0.035 m.

All walls were discretised uniformly. Geometrical convergence was tested for increasing number of cells (12 cells in each edge being enough).

Fig. 3 shows two planes A (z = 0.004 m) and B (x = 0.004 m) where we determined distribution of potential from the precomputed surface charge density by means of analytical expressions. The program was written in MATLAB.

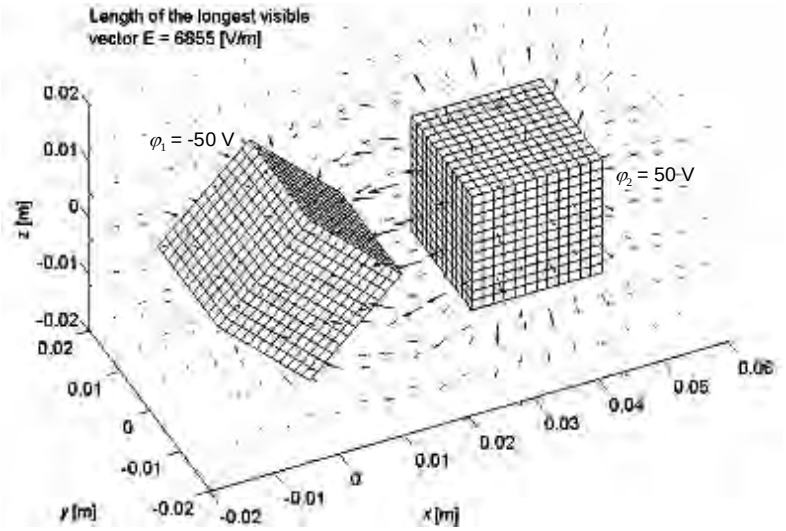

Fig. 2. Arrangement of the charged cubes

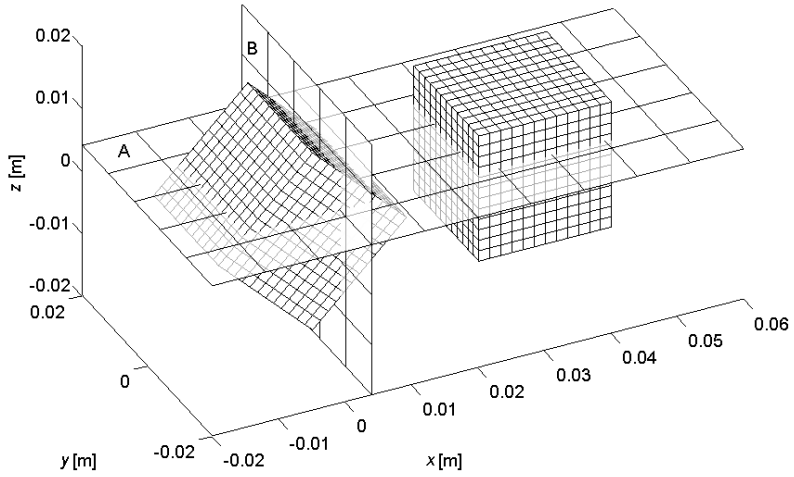

Fig. 3. Two planes with calculated potential distribution

Fig. 4 depicts distribution of the electric potential in plane A obtained from values of the potential at a relatively large set of selected points. The equipotential lines consisting of short straight lines were constructed by means of a linear interpolation. Fig. 5 contains distribution of the same quantity and electric field strength along the abscissa between points M and N representing the centres of the nearest parallel edge and side of both cubes. Obvious is inaccuracy at point M (there is about -46 V instead of -50 V). This inaccuracy caused by using low degree polynomial substitution of the surface density in each cell and round-off errors is the smaller the finer mesh we use. Particular components of the electric field strength at any selected point were calculated directly from the distribution of charges, which provides much more accurate results in comparison with their calculation from the potential. However, computation of this quantity requires a lot of additional operations associated with necessary co-ordinate transformations and takes a considerable amount of time. The results are in Fig. 2.

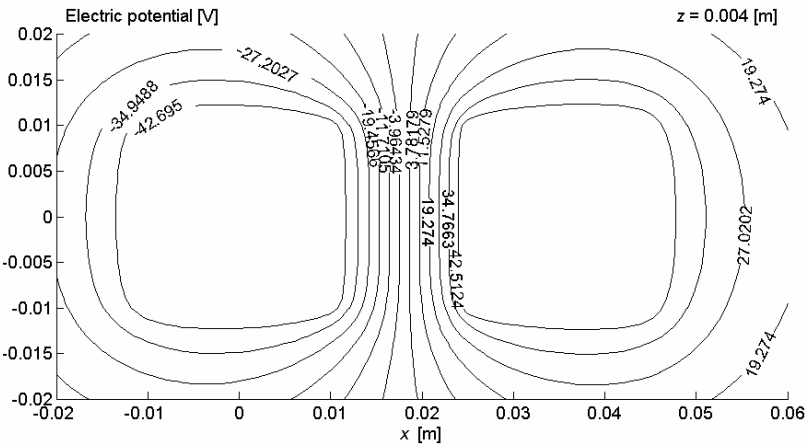

Fig. 4. Distribution of electric potential in plane A

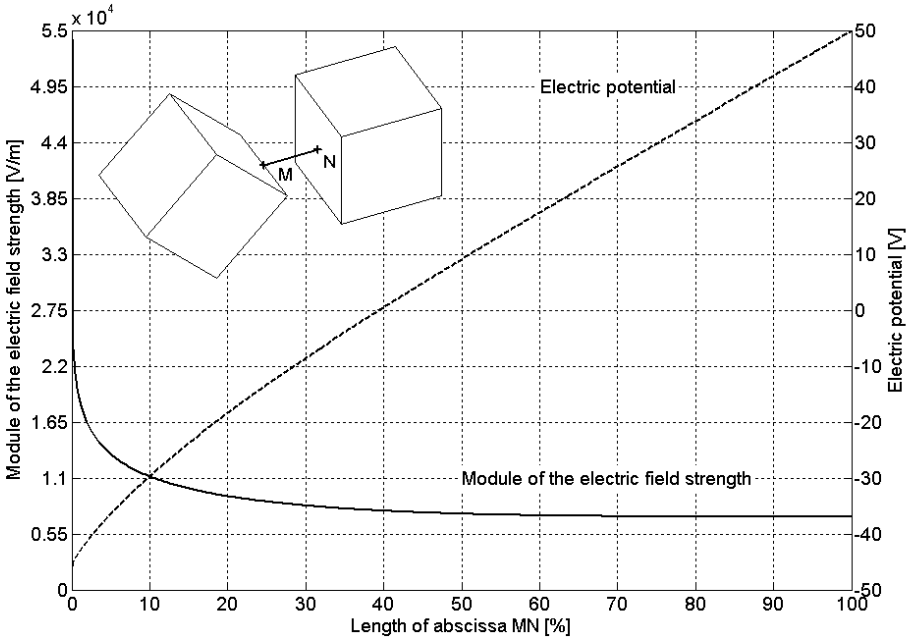

Fig. 5. Distribution of potential and electric field strength along abscissa MN

Special model. Let us consider a system of n charged 1D filaments Ω_i of general shape (Fig. 6) carrying potentials φ_i, $i = 1,..., n$. The filaments are placed in an isotropic medium of relative permittivity ε_r. The task is to find distribution of the electric field in such a system.

The thin conductors are first replaced by a set of point charges (conductor Ω_1 by charges $Q_{11},..., Q_{1k1}$, conductor Ω_2 by charges $Q_{21},..., Q_{2k2}$ etc. located along helicoidal curves surrounding the filaments). While position of particular point charges can be to some extent arbitrary, their values are determined from the condition that they produce the prescribed potential along the original filaments. Let us further choose (Fig. 6) points $P_{11},..., P_{1k1}$ located on conductor Ω_1, $P_{21},..., P_{2k2}$ on conductor Ω_2 etc. Even when these points may be selected relatively arbitrarily, we used the perpendicular projections of corresponding points $Q_{11},..., Q_{1k1}$ to conductor Ω_1, $Q_{21},..., Q_{2k2}$ to conductor Ω_2 etc. For any point P_{ml} where $m \in \langle 1, n \rangle$ and $l \in \langle 1, k_m \rangle$ of this set we can write

discrete equation

$$\varphi_m\left(P_{ml}\right)=\frac{1}{4\pi\varepsilon_0}\cdot\sum_{i=1}^{n}\sum_{j=1}^{k_j}\frac{Q_{ij}}{\left|r_{Q_{ij}}-r_{P_{ml}}\right|} \tag{4}$$

where φ_m denotes potential of the m-th conductor and expression in the absolute value in the denominator the distance between the charge Q_{ij} and point P_{ml}. The system of equations (4) provides the values of charges Q_{ij} that are immediately used for consequent computations of the field quantities all over the investigated area.

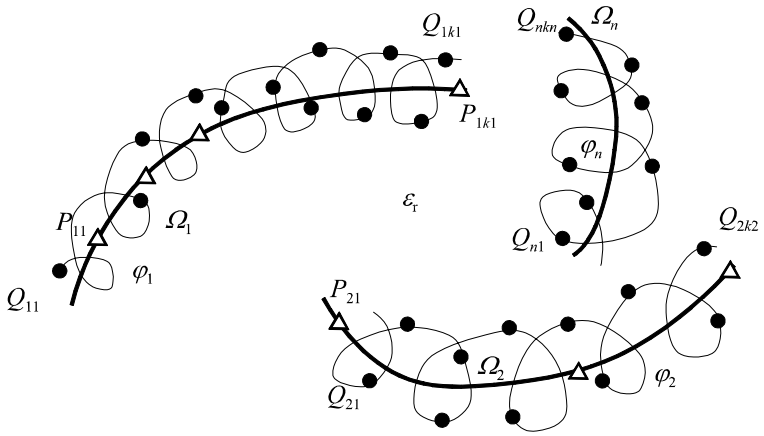

Fig. 6. The solved arrangement

Geometrical convergence of the algorithm was tested on a thin direct conductor of length l = 100 m carrying potential φ = 1 V (infinity is characterised by potential φ = 0 V). Solution to the system (4) provides distribution of the point electric charges along a conductor (see Fig. 7, a, b). Fig. 8 depicts distribution of the radial component E_r of the electric field strength. We can see that near the conductor its distribution fails, but at a distance higher than 0.1 m from the conductor the difference between the real and calculated distribution is almost negligible (which corresponds with expectations). Parameters substantially affecting limits of the method are the number of substituting point charges and radius of the selected helix. Computations were realized by a code written in Borland Delphi.

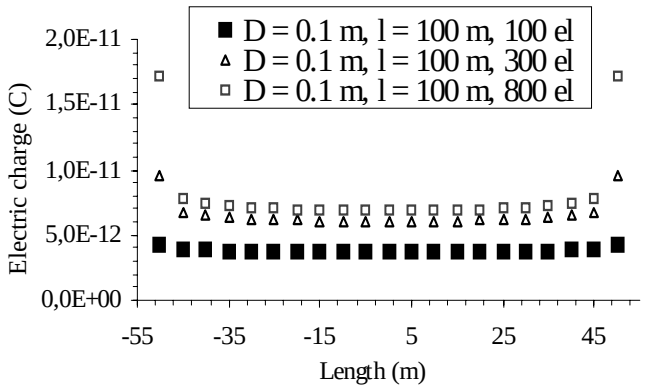

Fig. 7a. Distribution of the electric charge along the conductor (for 800 point charges and more the results are practically equal)

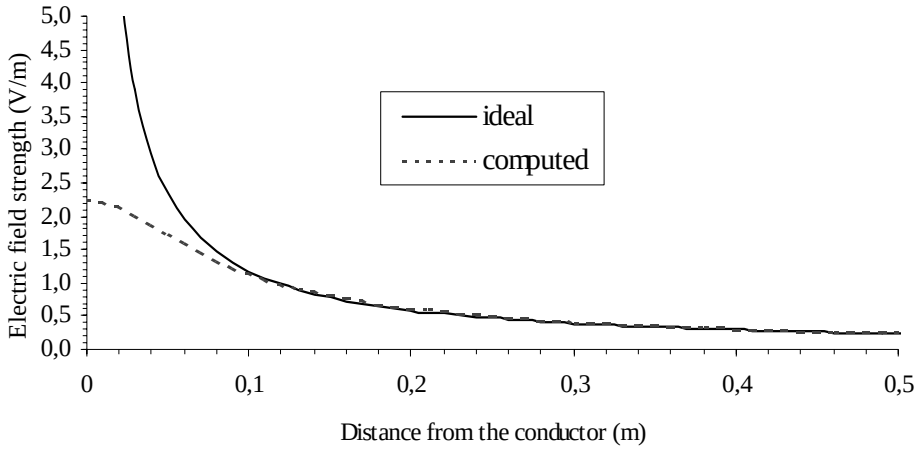

Fig. 7b. Radial component E_r of the electric field strength versus distance from the conductor in the plane perpendicular to the conductor in its centre

Illustrative example. The algorithm was used for mapping electric field near the crossing of two three-phase lines of high voltage with potentials 110 kV and 10.5 kV, respectively. Arrangement and dimensions are obvious from Figs. 8 and 9. The sequence of phases in both lines is the same and there is no phase shift between them.

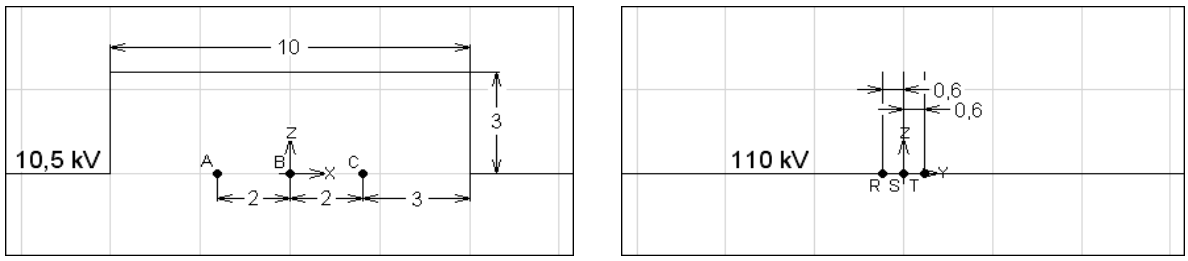

Fig. 8. Arrangement and dimensions of particular conductors (front and side views)

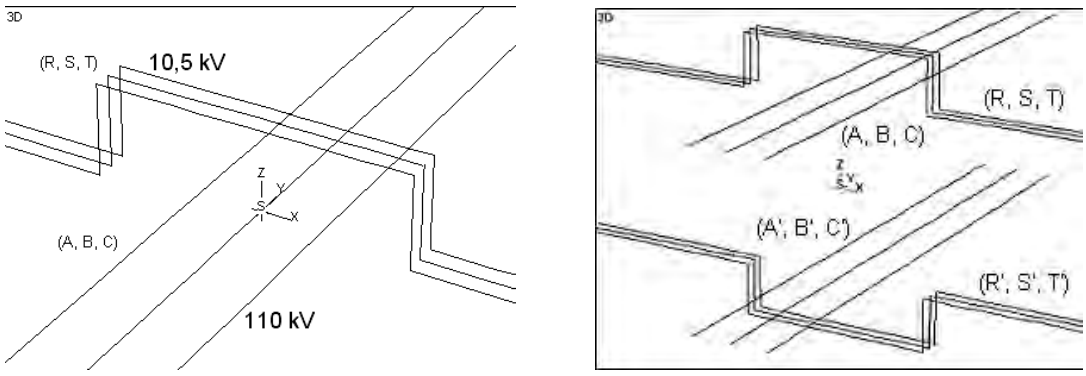

Fig. 9. 3D view of the arrangement and influence of the earth

The length of the input conductors to the crossing was selected with respect to the geometrical convergence. The convergence was evaluated in terms of contribution of length of the input conductor to the resultant distribution of the electric field strength. The arrangement contains 9000 charges. The influence of the earth with zero potential in the plane *xy* was respected by

means of mirroring of the main lines by lines with opposite potentials. The line with potential 110 kV is 5 meters above the earth.

Fig. 10 shows distribution of electric field strength above lines with potential 110 kV for time t = 0 s and plane yz (x = 0) m. There is practically no influence of the second 10.5 kV line. The field is computed for the following parameters:

	110 kV			10.5 kV		
phase	A	B	C	R	S	T
U (kV)	0	95.262	-95.262	0	9.093	-9.093

Distribution of electric field strength along axis x at time t = 0 s is shown in Fig. 11.

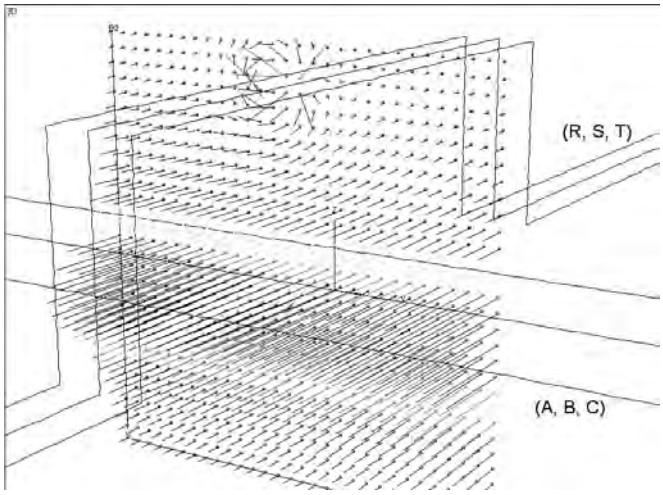

Fig. 10. Distribution of electric field in plane yz, t = 0 s

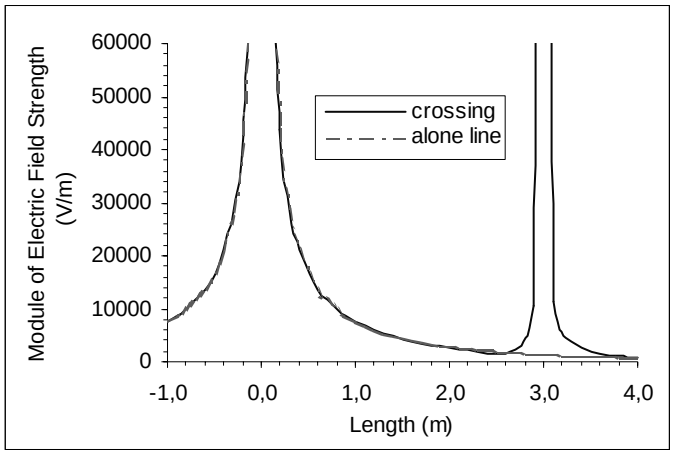

Fig. 11: Distribution of electric field strength along axis x for time t = 0 s (compared with alone line with potential 10.5 kV)

Conclusion. Both discussed methods can significantly help with mapping of large electric fields where classic FD or FE-based techniques may fail. In the continuation of the work, however, it is necessary to improve some parts of the presented algorithms. As for integral methods, important is particularly selection of high-degree polynomials substituting the charge density in the cells providing good approximation of its distribution especially near the corners and edges of the

charged bodies. The most serious aspect of the second method is the mathematical evaluation of selection of positions of individual point charges Q_{ij} and checkpoints P_{ij}. Optimization of their selection would surely contribute not only to their decrease (leading to system matrix of lower order) but also to higher accuracy of results.

Acknowledgement. This work has been financially supported from the Research Plans MSM 232200008 and MSM 212300016.

1. Ida, N. Engineering Electromagnetics. Springer-Verlag, New York, Inc., 2001. 2. Chari, M. V. K., Salon, S.J. Numerical Methods in Electromagnetism, Academic Press, San Diego, 2000. 3. Doležel, I., Kloucek, P., Šolín, P., Ulrych, B. Distribution of Electrical Charge in a System of Finite Conductors. Acta Technica CSAV 48, 2003. – P. 1–13.

УДК 519.62 – 519.711 : 621.34

В.І. Мороз
Національний університет “Львівська політехніка”

ПОГЛЯД ІНЖЕНЕРА-ЕЛЕКТРИКА НА ЧИСЛОВІ МЕТОДИ РОЗВ'ЯЗУВАННЯ ЗВИЧАЙНИХ ДИФЕРЕНЦІАЛЬНИХ РІВНЯНЬ

У статті розглянуті властивості числових методів розв’язання звичайних диференціальних рівнянь, що описують моделі електроприводів.

There were analysed properties of the numeric methods for solving the ordinary differential equations that described the electric drives control systems.

Постановка проблеми. Завдяки розвитку комп’ютерної техніки переважна більшість технічних рішень обов’язково проходить етап комп’ютерного моделювання для перевірки їх правильності чи ефективності. Одним з визначальних етапів комп’ютерного моделювання є застосування числових методів для знаходження шуканого розв’язку. Зокрема, для розрахунку динаміки застосовуються числові методи розв’язування звичайних диференціальних рівнянь. У сукупності з математичною моделлю об’єкта вони утворюють комп’ютерну модель, поведінка якої визначається дією обох компонентів.

Традиційно склалося, що особливості числових методів розв’язування звичайних диференціальних рівнянь не враховуються – вважається, що вони мало впливають на поведінку результуючої комп’ютерної моделі. Цю ілюзію особливо підсилюють сучасні алгоритми з автоматичним вибором кроку інтегрування, наприклад, застосовані у математичному пакеті MATLAB і його додатку – пакеті Simulink. Не применшуючи позитивних якостей Simulink (дуже зручний засіб для візуального імітаційного моделювання, зокрема, електроприводів), слід відзначити, що це середовище створює враження легкого розв’язання будь-якої задачі, яку можна подати структурною схемою з елементів Simulink. Майже десяток доступних реалізацій числових методів для розв’язування диференціальних рівнянь з автоматичним вибором кроку, що наявні в Simulink, ніби переконують у всесильності сучасної комп'ютерної науки. У той самий час ейфорія триває недовго – досить розпочати моделювання системи з жорсткими